Inorg. Chem. **1994,** *33,* 6101−6110

Heteronuclear Complexes Derived from *trans*-a_2PtL_2 (a = NH_3 or CH_3NH_2, L = 2-Pyridonate). Distorted Coordination Geometries of All Three Metals in *trans*-$[a_2PtL_2CuL_2Pt(a_2)]^{2+}$ and an Extraordinary Short Hydrogen Bond in *trans*-$[a_2PtL(LH)]^+$

André Schreiber,[1a] Olga Krizanovic,[1a] Edda Claudia Fusch,[1a] Bernhard Lippert,*,[1a] Francesca Lianza,[1b] Alberto Albinati,*,[1b] Stuart Hill,[1c] David M. L. Goodgame,*,[1c] Horst Stratemeier,[1d] and Michael A. Hitchman*,[1d]

Fachbereich Chemie, Universität Dortmund, 44221 Dortmund, Germany, Istituto Chimico Farmaceutico della Università di Milano, 20131 Milano, Italy, Chemistry Department, Imperial College, London SW7 2AY, England, and Chemistry Department, University of Tasmania, Hobart, Tasmania 7081, Australia

Received December 15, 1993[⊗]

trans-$[a_2PtL(LH)]NO_3 \cdot xH_2O$ (a = NH_3, L = 2-pyridonate, C_5H_4NO, LH = 2-hydroxypyridine, C_5H_5NO, $x = 2$ (**1**); a = CH_3NH_2, $x = 0$ (**2**)) have been prepared, and Cu^{II} adducts of composition *trans*-$[a_2PtL_2CuL_2Pta_2](NO_3)_2$ (a = NH_3 (**3**); a = CH_3NH_2 (**4**)) have been isolated. X-ray structures of **2**, **3**, and **4** are reported. Crystal data are as follows: **2**, orthorombic system, space group *Pccn*, $a = 8.486(1)$ Å, $b = 13.200(3)$ Å, $c = 13.920(1)$ Å, $Z = 4$; **3**, orthorombic, space group *Fdd*2, $a = 23.281(4)$ Å, $b = 22.551(4)$ Å, $c = 10.852(2)$ Å, $Z = 8$; **4**, monoclinic system, space group $P2_1/n$, $a = 11.448(4)$ Å, $b = 18.771(2)$ Å, $c = 16.085(3)$ Å, $\beta = 105.81(2)°$, $Z = 4$. The cation of **2**, in which the two heterocyclic ligands bind to Pt via N(1) positions and adopt a coplanar *head−tail* arrangement, is structurally not unusual. In the crystal, cations of **2** are associated by very short intermolecular H bonds of 2.443(9) Å into infinite chains. Since the acidic proton of this H bond was not located, a differentiation between a symmetric single minimum H bond and a double minimum situation (with H disordered) was not possible, but IR spectroscopy (no deuterium shift of $\nu(OH)$ at ca. 750 cm^{-1}) favors the latter. The Cu^{II} ions in **3** and **4** are coordinated via O(2) oxygens of the four 2-pyridonato ligands. Geometries and several spectroscopic properties of **3** and **4** differ markedly from the corresponding complexes of composition *cis*-$[a_2Pt(L')_2Cu(L')_2Pta_2]^{2+}$ (L′ = bridging pyrimidine nucleobase; coordination of Pt via endocyclic ring N, of Cu via exocyclic O) in the following ways: Coordination spheres of both Pt^{II} and Cu^{II}, which are essentially square-planar in the *cis*-compounds, have undergone considerable distortions in **3** and **4**. Pt−Cu distances in **3** (2.6312(4) Å) and **4** (2.6320(8) and 2.6450(8) Å) are significantly shorter. The *trans*-compounds **3** and **4** are of orange-red colors and exhibit d−d transitions at considerably lower energy than the *cis*-compounds which are greenish. EPR spectra (*g* values, *A* values) are also different and the powder spectrum of **3** is unusual, being a superposition of signals due to the molecular **g**-tensor, and weak peaks due to an exchange-narrowed **g**-tensor.

Heteronuclear Pt_nCu ($n = 1, 2$) complexes derived from *cis*-a_2PtL_2 or *cis*-$[a_2PtLL']^+$ (a = NH_3 or a_2 = *N,N,N′,N′*-tetramethylethylenediamine, L = 1-methyluracil,[2−4] L′ = 1-methylcytosine,[5] 7.9-dimethylhypoxanthine[6]) display characteristic greenish colors and have square-planar or tetragonally elongated coordination spheres about the Cu.[7] Despite an essentially constant bite distance of the nucleobase, e.g. N(3)−O(4) in 1-methyluracil compounds, the possibility of the metal planes to tilt with respect to each other, permits a rather flexible arrangement of the CuO_4 plane (Chart 1, a and b). Consequently, intracomplex Pt−Cu distances vary between 2.681(1) Å [5] and 2.9843(1) Å [4] and are markedly influenced by the bulk of the amine ligands at the Pt.

Chart 1

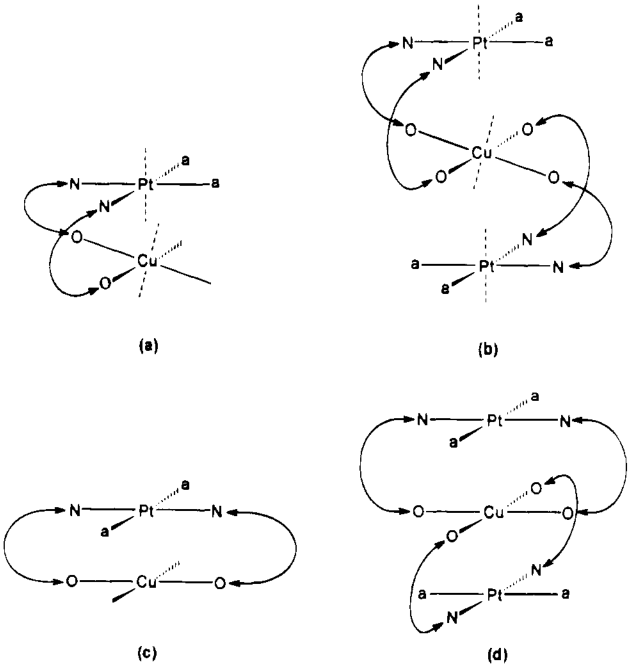

[⊗] Abstract published in *Advance ACS Abstracts,* November 1, 1994.

(1) (a) Universität Dortmund. (b) Università di Milano. (c) Imperial College London. (d) University of Tasmania.

(2) Neugebauer, D.; Lippert, B. *J. Am. Chem. Soc.* **1982**, *104*, 6596.

(3) Mutikainen, I.; Orama, O.; Pajunen, A.; Lippert, B. *Inorg. Chim. Acta* **1987**, *137*, 189.

(4) Frommer, G.; Lianza, F.; Albinati, A.; Lippert, B. *Inorg. Chem.* **1992**, *21*, 2434.

(5) Lippert, B.; Thewalt, U.; Schöllhorn, H.; Goodgame, D. M. L.; Rollins, R. W. *Inorg. Chem.* **1984**, *23*, 2807.

(6) Lippert, B. *Prog. Inorg. Chem.* **1989**, *37*, 1.

(7) Goodgame, D. M. L.; Hitchman, M. A.; Lippert, B. *Inorg. Chem.* **1986**, *25*, 2191.

0020-1669/94/1333-6101$04.50/0

Extending our studies to derivatives of *trans*-a_2PtL_2 (Chart 1, c and d), we reasoned that the steric constraint of the bite distance of the heterocycle in such compounds might impose a severe distortion on the heterometal and/or the Pt coordination geometry. The unexpected light-orange color or *trans*-$[(CH_3NH_2)_2Pt(urd)_2Cu(urd)_2Pt(CH_3NH_2)_2]^{2+}$ (urd = uridine)[8] seemed to further support this view. Moreover, findings with related dinuclear complexes derived from *trans*-a_2Pt (1-MeC^-)$_2$ (1-MeC^- = 1-methylcytosine deprotonated at N(4)) and heterometals such as Pd(II)[9] or Hg(II)[10] had revealed that in these compounds Pt acted as a ligand of the heterometal, thereby avoiding the need to accommodate one additional ligand at the heterometal. Interestingly, analogous Pd_2 complexes have not been isolated as yet; rather, the (compared to PtPd) kinetically more labile system escapes the steric clash between amine ligands at the two metal centers by isomerization of both Pd entities from *trans* to *cis* geometries.[11]

This work on heteronuclear Pt_2Cu complexes obtained from *trans*-a_2PtL_2 (L = 2-pyridonate) was prompted by our findings with the corresponding uridine complex. It provided a test for the effects of the amine ligands in *trans*-a_2PtL_2 on the coordination geometry of Cu(II) when bound to L at short distance from Pt.

Experimental Section

trans-$[(NH_3)_2Pt(C_5H_4NO)(C_5H_5NO)]NO_3 \cdot 2H_2O$, **1**, was prepared by reacting *trans*-$[(NH_3)_2Pt(H_2O)_2]^{2+}$, obtained *in situ* from *trans*-$(NH_3)_2PtCl_2$[12] and $AgNO_3$ with 2 equiv of 2-pyridone (2-hydroxypyridine) at pH 5−6 (2 d, 50 °C), evaporation to dryness and recrystallization from water (yield 25%). **1** crystallized as slightly yellow columns. Anal. Calcd (found) for $C_{10}H_{19}N_5O_7Pt$: C, 23.26 (23.15); H, 3.70 (3.80); N, 13.56 (13.85). IR (cm^{-1}): 3300 s, b, 1620 vs, 1540 w, 1510 vs, 1445 m, 1386 vs, 1310 vs, 1155 m, 1120 m, 1025 m,sh, 852 m, 780 s, 741 m, 590 w,sh.

trans-$[(CH_3NH_2)_2Pt(C_5H_4NO)(C_5H_5NO)]NO_3$, **2**, was prepared in a similar way from *trans*-$(CH_3NH_2)_2PtCl_2$[13] and 2-hydroxypyridine. The reaction conditions were the same as described above and the obtained product (yield 66%) was recrystallized from water at 4 °C and isolated as slightly yellowish cubes. Anal. Calcd (found) for $C_{12}H_{19}N_5O_5Pt$: C, 28.35 (28.10); H, 3.78 (3.80); N, 13.80 (13.90). IR (cm^{-1}): 3251 s, 3130 m, 3021 w, 2994 w, 2952 w, 1650 m, 1603 s, 1539 m, 1527 w, 1447 s, 1381 vs, 1350 vs, 1326 vs, 1272 s, 1164 m, 1119 s, 1089 s, 1058 s, 1026 m, 961 m, 860 s, b. Superimposed on these bands is an extremely intense and broad band centered at ca. 750 cm^{-1}. It is tentatively assigned to ν(OH). Upon deuteration, this band is not shifted (cf. Results and Discussion).

trans-$[(NH_3)_2Pt(C_5H_4NO)_2Cu(C_5H_4NO)_2Pt(NH_3)_2](NO_3)_2$, **3**, was prepared as follows: **1** (0.25 mmol) was dissolved in water (10 mL), the pH raised from 3.9 to 8.0 by means of NaOH, and $Cu(NO_3)_2 \cdot 3H_2O$ (0.25 mmol) was added. From the intensively red solution, orange-red crystals were obtained in 25% yield upon slow evaporation of the solution at 4 °C. Anal. Calcd (found) for $C_{20}H_{28}N_{10}O_{10}Pt_2Cu$: C, 23.49 (23.60); H, 2.76 (2.90); N, 13.70 (13.85). IR (cm^{-1}): 3400 s, 3350 s, 3270 s, 3200 s, 1660 vs, 1590 vs,sp, 1525 vs, 1510 vs, 1482 vs, 1430 vs, 1390 vs, 1370 vs, 1360 vs, 1345 m, 1205 m, 1195 m, 1160 s, 1075 s, 898 vs, 890 vs, 840 s, 820 vs, 790 s, 780 s, 630 vs.

trans-$[(CH_3NH_2)_2Pt(C_5H_4NO)_2Cu(C_5H_4NO)_2Pt(CH_3NH_2)_2](NO_3)_2$, **4**, was obtained as follows: A solution of **2** (0.098 mmol) in water (5 mL) was brought to pH 8.3 by means of NaOH. Subsequently solid $Cu(NO_3)_2 \cdot 3H_2O$ (0.098 mmol) was added. From the red solution the product crystallized at 4 °C as orange-red cubes (yield 35%). IR (cm^{-1}): 3220 s, b, 1623 s, 1551 m, 1494 s, 1453 s, 1360 s, b, 1159 m, sh, 1126 w, 1112 m, 1039 m, 865 s, 834 w, 799 m, 783 m, 753 w, 597 m, 543 w.

Table 1. Experimental Data for the X-ray Diffraction Study of Compounds **2−4**

	compound		
	2	**3**	**4**
chem formula	$C_{12}H_{19}N_5O_5Pt$	$C_{20}H_{28}CuN_{10}O_{10}Pt_2$	$C_{24}H_{28}CuN_{10}O_{10}Pt_2$
mol wt	508.41	1022.23	1070.27
T, °C	23	23	23
space group	*Pccn* (No. 56)	*Fdd*2 (No. 43)	$P2_1/n$ (No. 14)
a, Å	8.486(1)	23.281(4)	11.448(4)
b, Å	13.200(3)	22.551(4)	18.771(2)
c, Å	13.920(1)	10.852(2)	16.085(3)
β, deg			105.81(2)
V, Å^3	1559.2(4)	5697(3)	3326(1)
Z	4	8	4
ϱ(calcd), g cm^{-3}	2.166	2.383	2.137
μ, cm^{-1}	91.234	107.116	91.802
λ, Å	0.710 69 (graphite monochromated)		
θ range, deg	$2.5 < \theta < 25.0$	$2.5 < \theta < 25.0$	$2.5 < \theta < 27.0$
transm coeff.	0.7720−1.1453	0.8395−0.9952	0.8283−0.9993
f	0.030	0.045	0.040
R^a	0.016	0.030	0.025
$R_w{}^b$	0.024	0.038	0.033

[a] $R = \sum(||F_o| - (1/k)|F_c||)/\sum|F_o|$. [b] $R_w = [\sum w(|F_o| - (1/k)|F_c|)^2/\sum w|F_o|^2]^{1,2}$, where $w = [\sigma^2(F_o)]^{-1}$; $\sigma(F_o) = [\sigma^2(F_o^2) + f^2(F_o^2)]^{1/2}/2F_o$.

Spectroscopy and Other Measurements. ^1H NMR spectra of **1** and **2** were recorded on a Bruker AC200 in D_2O (internal TSP as reference). IR spectra (KBr) were taken on a Perkin-Elmer 580B, Raman spectra (solid state) on a Coderg T800 spectrometer with Ar^+ laser excitation (514.5 nm). Measurements of powder EPR spectra at Q-band frequency and of the electronic spectra of the polycrystalline samples were made as described previously.[5,7] Crystals of **3** for EPR and optical measurements were selected under a microscope. The Q-band crystal and X-band powder EPR measurements were made on a JEOL JES-FE spectrometer. The electronic spectrum of a single crystal were recorded on a Cary 5 spectrophotometer, with the sample cooled using a cryodyne 22 C cryostat.

Potentiometric titrations were carried out by use of an automated titroprocessor (Methrohm, mode 686) and a combination glass electrode.

X-ray Crystallography. X-ray structure analyses were performed for **2**, **3**, and **4**. All crystals were mounted on glass fibers, at a random orientation, on an Enraf-Nonius CAD4 diffractometer for the unit cell and space group determinations and for the data collections. Unit cell dimensions were obtained by least squares fit of the 2Θ values of 25 high order reflections ($9.0 < \Theta < 15.7°$ for **2**, $9.1 < \Theta < 14.8°$ for **3** and $9.5 < \Theta < 16.9°$ for **4**, respectively) using the CAD4 centering routines. Selected crystallographic and other relevant data are listed in Table 1 and supplementary Table S1.

Data were measured with variable scan speed to ensure constant statistical precision on the collected intensities. Three standard reflections were used to check the stability of the crystal and of the experimental conditions and measured every hour. The orientation of the crystal was checked by measuring three reflections every 360 measurements. Data have been corrected for Lorentz and polarization factors using the data reduction programs of the MOLEN package.[14] Empirical absorption corrections were applied to the data sets by suing azimuthal (Ψ) scans of "high-χ" angle reflections (three reflections having $\chi > 84°$, $13.1 < \Theta < 18.4°$ for **2**, four reflections with $\chi > 85°$, $13.2 < \Theta < 17.0°$ for **3** and two reflections having $\chi > 88°$, $12.6 < \Theta < 18.1°$ for **4**).

The standard deviations on intensities were calculated in terms of statistics alone, while those on F_o were calculated as shown in Table 1 and Table S1.

---

[8] (a) Dieter, I.; Lippert, B.; Schöllhorn, H.; Thewalt, U. *Z. Naturforsch.* **1990**, *45b*, 731. (b) Schöllhorn, H.; Thewalt, U.; Lippert, B. *J. Chem. Soc., Chem. Commun.* **1984**, 769.

[9] (a) Krumm, M.; Lippert, B.; Randaccio, L.; Zangrando, E. *J. Am. Chem. Soc.* **1991**, *113*, 5129. (b) Krumm, M.; Zangrando, E.; Randaccio, L.; Menzer, S.; Lippert, B. *Inorg. Chem.* **1993**, *32*, 700.

[10] Krumm, M.; Zangrando, E.; Randaccio, L.; Menzer, S.; Danzmann, A.; Holthenrich, D.; Lippert, B. *Inorg. Chem.* **1993**, *32*, 2183.

[11] Krumm, M.; Mutikainen, I.; Lippert, B. *Inorg. Chem.* **1991**, *30*, 884.

[12] Kaufmann, G. B.; Cowan, D. O. *Inorg. Synth.* **1963**, *7*, 239.

[13] Arpalahti, J.; Lippert, B.; Schöllhorn, H.; Thewalt, U. *Inorg. Chim. Acta* **1988**, *153*, 45.

[14] *MOLEN: Molecular Structure Solution Procedure*; Enraf-Nonius: Delft, The Netherlands, 1990.

Table 2. Atomic Positional Parameters for Compound **2**

atom	*x*	*y*	*z*	*B*,[a] Å^2
Pt	0.000	0.000	0.500	1.427(4)
O1	−0.250	−0.250	0.1645(2)	4.1(1)
O2	0.3571(5)	−0.0077(2)	0.5064(2)	2.81(8)
O3	−0.2598(5)	−0.1695(3)	0.2973(2)	5.30(8)
N1	−0.1521(4)	0.0470(3)	0.3975(2)	1.60(6)
N2	−0.0968(4)	−0.1426(3)	0.4922(2)	1.90(7)
N3	−0.250	−0.250	0.2523(2)	2.5(1)
C2	−0.3102(4)	0.0440(3)	0.4115(2)	2.06(8)
C3	−0.4117(4)	0.0782(4)	0.3395(3)	2.24(8)
C4	−0.3546(5)	0.1116(4)	0.2552(2)	3.0(1)
C5	−0.1925(6)	0.1145(4)	0.2399(2)	3.1(1)
C6	−0.0972(5)	0.0829(4)	0.3116(3)	2.39(8)
C7	0.0124(5)	−0.2293(5)	0.4886(3)	2.9(1)

[a] Anisotropically refined atoms are given in the form of the isotropic equivalent displacement parameter defined as $(4/3)[a^2\beta(1,1) + b^2\beta(2,2) + c^2\beta(3,3) + ab(\cos\gamma)\beta(1,2) + ac(\cos\beta)\beta(1,3) + bc(\cos\alpha)\beta(2,3)]$.

Table 3. Atomic Positional Parameters for Compound **3**

atom	*x*	*y*	*z*	*B*,[a,b] Å^2
Pt	0.92537(1)	1.08749(1)	0.9700(2)	1.467(6)
Cu	1.000	1.000	0.960	1.64(3)
O2	0.9457(4)	0.9712(3)	0.8368(8)	2.4(2)
O2a	1.0370(3)	1.0491(3)	1.0873(9)	2.4(2)
N1	0.9064(3)	1.0630(4)	0.7960(7)	1.4(2)
N1a	0.9560(4)	1.1033(4)	1.1423(8)	1.7(2)
N2	0.8664(4)	1.0289(4)	1.038(1)	2.5(2)
N3	0.9849(4)	1.1440(4)	0.901(1)	2.5(2)
C2	0.9239(4)	1.0088(5)	0.758(1)	1.7(2)
C2a	1.0094(5)	1.0777(5)	1.169(1)	1.8(2)
C3a	1.0317(6)	1.0856(5)	1.289(1)	2.7(3)
C3	0.9184(5)	0.9932(6)	0.633(1)	2.7(2)
C4	0.8945(6)	1.0326(6)	0.551(1)	3.1(3)
C4a	1.0031(6)	1.1196(6)	1.372(1)	3.2(3)
C5	0.8750(6)	1.0869(5)	0.592(1)	2.9(3)
C5a	0.9512(6)	1.1459(6)	1.342(1)	3.3(3)
C6a	0.9304(4)	1.1368(5)	1.226(1)	2.7(2)
C6	0.8820(4)	1.1007(5)	0.713(1)	2.4(2)
N4	0.9869(5)	1.2709(5)	1.093(1)	3.1(2)
O3	1.0256(5)	1.2340(5)	1.096(2)	6.0(3)
O4	0.9907(7)	1.3166(6)	1.152(1)	7.0(3)
O5	0.9442(5)	1.2599(4)	1.029(1)	4.2(2)

[a] See footnote *a* of Table 2. [b] N4, O3, O4, O5 denote nitrate atoms.

The structures were solved by a combination of Patterson and Fourier methods and refined by full matrix least-squares[14] (the function minimized being $\Sigma[w(F_o - 1/kF_c)^2]$). A type I isotropic extinction correction[15] was applied for compounds **2** and **3**. The scattering factors used, corrected for the real and imaginary parts of the anomalous dispersion were taken from ref 16. All calculations were carried out using the Enraf-Nonius MOLEN package.[14]

Structural Study of 2. A total of 1695 independent data, obtained as described above (of which 821 were considered as observed having $|F_o|^2 > 3.0\sigma|F|^2$) were used for the refinement. These data were, at a later stage, corrected empirically for absorption using the program DIFABS.[17] For the final refinement anisotropic temperature factors were used for all atoms except the hydrogens, their contribution, in calculated positions (C−H = 0.95 (Å), $B(H) = 1.3B(C_{bonded})$ (Å^2)), being taken into account but not refined. Final atomic coordinates and equivalent isotropic displacement parameters are given in Table 2.

Structural Study of 3. Of the 1396 independent data collected, 1298 were considered having $|F_o|^2 > 2.5\sigma|F|^2$. The structure was refined as described above, using anisotropic temperature factors for all atoms. The handedness of the crystal was tested by refining the two possible sets of coordinates; those giving the lowest R_w factors[18] are listed in Table 3.

Table 4. Atomic Positional Parameters for Compound **4**

atom	*x*	*y*	*z*	*B*,[a,b] Å^2
Pt1	0.92165(2)	0.22040(1)	0.24341(1)	2.565(4)
Pt2	0.68926(2)	0.18039(1)	0.48107(1)	2.596(4)
Cu	0.81199(6)	0.20370(4)	0.36713(4)	2.89(1)
O2′	0.6742(4)	0.2680(2)	0.3178(3)	4.09(9)
O2a	0.9144(4)	0.2868(3)	0.4166(3)	4.5(1)
O2	0.7365(4)	0.1235(2)	0.2922(3)	4.23(9)
O2a′	0.9332(4)	0.1424(3)	0.4447(3)	4.09(9)
N1a′	0.8176(4)	0.1063(3)	0.5337(3)	3.1(1)
N1′	0.5739(4)	0.2586(3)	0.4236(3)	2.93(9)
N1	0.8498(4)	0.1253(3)	0.1949(3)	2.88(9)
N1a	0.9883(4)	0.3135(3)	0.3013(3)	3.3(1)
N2′	0.5849(5)	0.0994(3)	0.4134(3)	4.1(1)
N2	0.7743(4)	0.2777(3)	0.1733(3)	3.5(1)
N3	1.0686(4)	0.1624(3)	0.3130(3)	3.5(1)
N3′	0.7942(5)	0.2604(3)	0.5514(3)	3.7(1)
C2′	0.5929(5)	0.2918(3)	0.3531(4)	3.2(1)
C2a	0.9740(6)	0.3288(3)	0.3805(4)	3.6(1)
C2	0.7670(5)	0.0940(3)	0.2301(4)	3.2(1)
C2a′	0.9230(5)	0.1069(3)	0.5102(4)	3.3(1)
C3a′	1.0213(6)	0.0668(3)	0.5604(4)	4.1(1)
C3a	1.0281(6)	0.3915(4)	0.4233(5)	4.5(2)
C3	0.7177(6)	0.0281(4)	0.1955(4)	4.2(1)
C3′	0.5240(6)	0.3518(4)	0.3200(4)	3.9(1)
C4a	1.0933(7)	0.4352(4)	0.3846(5)	5.2(2)
C4′	0.4352(6)	0.3755(4)	0.3543(4)	4.4(2)
C4	0.7512(7)	−0.0030(4)	0.1292(5)	4.9(2)
C4a′	1.0104(7)	0.0274(4)	0.6271(4)	5.0(2)
C5a	1.1049(6)	0.4187(4)	0.3046(5)	5.4(2)
C5	0.8379(6)	0.0303(4)	0.0956(4)	4.6(2)
C5′	0.4134(5)	0.3400(4)	0.4238(4)	4.2(1)
C5a′	0.8990(8)	0.0251(4)	0.6469(4)	5.1(2)
C6′	0.4849(5)	0.2828(3)	0.4569(4)	3.6(1)
C6a	1.0538(6)	0.3580(4)	0.2641(4)	4.3(1)
C6a′	0.8070(6)	0.0650(4)	0.5998(4)	4.2(1)
C6	0.8830(6)	0.0927(4)	0.1294(4)	3.7(1)
C7′	0.4760(7)	0.1147(5)	0.3403(5)	5.5(2)
C7	0.6860(7)	0.2412(5)	0.0973(5)	5.7(2)
C8	1.1803(6)	0.2001(5)	0.3632(5)	5.8(2)
C8′	0.8742(7)	0.2425(5)	0.6416(5)	5.7(2)
N4	0.3035(5)	0.5983(3)	0.3532(4)	4.6(1)
N5	1.3942(6)	0.0860(3)	0.5717(4)	5.2(1)
O3	0.3137(6)	0.5530(3)	0.2998(4)	8.3(2)
O4	0.3419(5)	0.6588(3)	0.3470(3)	5.7(1)
O5	0.2576(6)	0.5865(4)	0.4129(4)	8.7(2)
O6	1.3297(5)	0.0595(4)	0.6138(4)	7.6(2)
O7	1.4738(6)	0.0497(4)	0.5563(5)	13.0(2)
O8	1.3955(6)	0.1494(3)	0.5565(4)	7.8(2)

[a] See footnote *a* of Table 2. [b] N4, O3, O4, O5 and N5, O6, O7, O8 denote atoms of nitrate anions.

Structural Study of 4. A total of 7322 independent data were collected of which 4936 were used for the refinement, having $|F_o|^2 > 3.0\sigma|F|$. All atoms were refined anisotropically with the hydrogen atoms contribution added as above. Final atomic coordinates and equivalent displacement parameters are given in Table 4.

Results and Discussion

Starting Compounds. Compound **1** crystallizes in the form *trans*-$[(NH_3)_2Pt(C_5H_4NO)(C_5H_5NO)]NO_3 \cdot 2H_2O$, containing a neutral 2-hydroxypyridine and an anionic 2-pyridonato ligand. Pt binding is for both ligands via the endocyclic N, as evident from the ^1H NMR (D_2O), which displays three groups of aromatic resonances centered at 6.75 ppm (H3, H5), 7.68 ppm (H4), and 8.25 ppm (H6) with ^{195}Pt satellites ($^3J \approx 38$ Hz) for the latter. The weakly acidic proton of the 2-hydroxypyridine can be titrated with base to give the neutral compound *trans*-$(NH_3)_2Pt(C_5H_4NO)_2$, which was not isolated, however. Compound **2**, *trans*-$[(CH_3NH_2)_2Pt(C_5H_4NO)(C_5H_5NO)]NO_3$, crystallizes in the same fashion as **1** as the hemiprotonated form of *trans*-$(CH_3NH_2)_2Pt(C_5H_4NO)_2$. The aromatic protons in the ^1H NMR (D_2O, pD 4.3), appear in three groups (200-MHz) at *ca.*

---

(15) Becker, P. J.; Coppens, R. *Acta Crystallogr.* **1975**, *A31*, 417.
(16) *International Tables for X-ray Crystallography*; Kynoch: Birmingham, England, 1974; Vol. IV.
(17) Walker, N.; Stuart, D. *Acta Crystallogr.* **1983**, *A39*, 159.
(18) Hamilton, W. C. *Acta Crystallogr.* **1965**, *13*, 502.

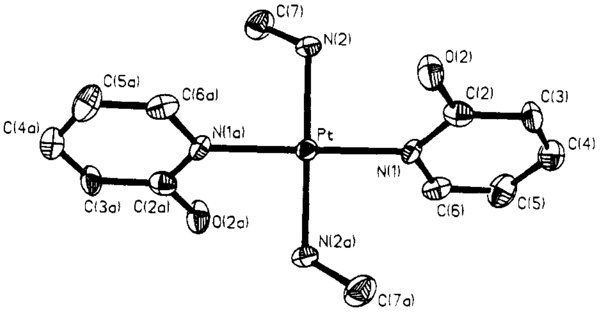

Figure 1. View of cation of *trans*-[(CH$_3$NH$_2$)$_2$Pt(C$_5$H$_4$NO)(C$_5$H$_5$NO)]-NO$_3$ (**2**) with atom-numbering scheme.

Table 5. Selected Bond Distances (Å) and Angles (deg) for **2**

Pt−N1	2.022(3)	N1−Pt−N1a	180.0(0)
Pt−N2	2.056(4)	N1−Pt−N2	89.4(1)
		N1−Pt−N2a	90.6(1)
N1−C2	1.357(5)	Pt−N2−C7	117.5(3)
N1−C6	1.367(6)	Pt−N1−C6	120.4(3)
C2−C3	1.396(6)	Pt−N1−C2	121.4(3)
C3−C4	1.344(6)	N1−C2−O2	116.1(5)
C4−C5	1.393(8)	C3−C2−O2	124.1(4)
C5−C6	1.350(7)	C2−N1−C6	118.2(1)
C2−O2	1.302(5)	N1−C2−C3	119.8(4)
N2−C7	1.473(7)	C3−C4−C5	119.9(5)
		N1−C6−C5	123.3(5)
		C2−C3−C4	120.7(4)
		C4−C5−C6	118.0(5)
O1−N3	1.222(5)	O1−N3−O3	120.4(3)
O3−N3	1.235(4)	O3−N3−O3a	119.2(6)
O3a−N3	1.236(5)	O3a−N3−O1	120.4(3)

6.8 ppm (H3,H5), 7.71 ppm (H4), and 8.37 ppm (H6), the latter with ^{195}Pt satellites ($^3J \approx 30$ Hz). Both the CH$_3$ (2.11 ppm, triplet prior to isotopic exchange NH$_2$ → ND$_2$) and NH$_2$ resonances of the methylamine ligands (4.54 ppm, broad singlet) display ^{195}Pt satellites of *ca.* 39 Hz (CH$_3$) and *ca.* 60 Hz (NH$_2$). The O−H proton in **2** has neither been detected in DMF-d_7 (insufficient solubility of **2**) nor in DMSO-d_6 (22 °C). DMSO causes displacement of 2-pyridone from **2** (5% within 15 min, 22 °C) with the NH proton of the free (neutral) ligand observable near $\delta = 11.5$ ppm at a later stage of the reaction. The pK_a of the acidic proton of **2** was determined by potentiometric titration with base and found to be 4.60 ± 0.05. This means that the N-platinated 2-pyridonato ligand in −**2** is more basic by almost 4 log units as compared to the free ligand (pK_a of protonated 2-pyridone is 0.75 [19]). The effect of the Pt electrophile on the H$^+$ affinity thus is comparable with that observed for *cis*-(NH$_3$)$_2$-Pt(1-MeU)$_2$ (pK_a of 1-MeUH$_2^+$, ≈−3; pK_a of *cis*-[(NH$_3$)$_2$Pt(1-MeU)(1-MeUH)]$^+$, +1.4 [20]). As with the protonated form(s) of *cis*-(NH$_3$)$_2$Pt(1-MeU)$_2$, the 2-hydroxypyridine ligands in **1** and **2** represent metalated forms of the rare tautomer of 2-pyridone.

Description of Cation of 2. Figure 1 depicts the cation of *trans*-[(CH$_3$NH$_2$)$_2$Pt(C$_5$H$_4$NO)(C$_5$H$_5$NO)]NO$_3$, **2**. Selected interatomic distances and angles are given in Table 5. The coordination sphere of Pt is close to ideal square-planar. Pt−N distances are normal.[13,21] The two heterocyclic ligands adopt a *head−tail* orientation and are coplanar. The methyl groups of the methylamine ligands are anti with respect to each other and both CH$_3$NH$_2$ groups are coplanar with Pt. Crystallographically, the two heterocycles are identical, meaning that the single proton of the 2-hydroxypyridine ligand is either centered between two cations or disordered over the two exocyclic oxygens, O(2) and O(2a) (vide infra). In either case the geometry of the two rings thus represents the mean of the anionic 2-pyridonate and the neutral 2-hydroxypyridine ligand, both platinated at the ring **N**. The effects of Pt binding to the nitrogen of both ligands on the geometry of the neutral 2-pyridone[22] have been discussed in detail.[21] A comparison of those bond lengths and angles of the 2-pyridonate ligand in *mer*-Pt(NH$_3$)$_2$Cl$_3$(C$_5$H$_4$NO)[21] and the 2-hydroxypyridine ligands in *cis*-[(NH$_3$)$_2$Pt(C$_5$H$_5$NO)$_2$]Cl$_2$[21] which differ significantly,[23] with corresponding data of **2** (Table 6), confirms the expected trend.

Cations of **2** are joined by very short intermolecular hydrogen bonds of 2.443(9) Å between O(2) sites of 2-hydroxypyridine and 2-pyridonato ligands (Figure 2). Infinite, planar (as far as Pt and the heterocyclic rings are concerned) zigzag chains are thus formed, which run along the x axis, and are arranged like tiles on a roof (supplementary material). The oxygens of nitrate anions form long contacts (3.076(5), 3.071(6) Å) with the protons of the methylamine nitrogens.

The H Bond in 2. Although the proton between O(2) and O(2a) of adjacent cations of **2** was not located, the shortness of the O•••O separation qualifies this H bond as of extraordinary strength. It certainly is among the strongest OH•••O bonds reported.[24]

In the IR spectrum of **2**, a very intense, broad band, ranging from ca. 950 cm^{-1} to 550 cm^{-1} and centered around 750 cm^{-1} is observed, which is superimposed on other, sharp bands. In agreement with observations in related, very strong O-H•••O bonded systems,[25] we assign this band to the ν(OH) mode. This band appears not to be affected upon deuteration, hence $\varrho = \nu(\mathrm{OH})/\nu(\mathrm{OD}) = 1$. Similar findings have been made in strongly H bonded systems having asymmetrical H bonds.[26] On the basis of its IR spectrum we therefore favor the view that the crystallographically symmetrical H bond in **2** is in fact not a symmetric single minimum H bond but rather a H bond with two narrowly spaced minima. We hope to eventually clarify this question unambiguously applying neutron diffraction.

Attempts to use Raman spectroscopy to obtain an answer were ambiguous: Although we have previously demonstrated the usefulness of Raman spectroscopy for studying tautomer equilibria,[27] linkage isomerism,[28] and the protonation state of metalated nucleobases,[20] inspection of the Raman spectrum (solid state) of **2** failed to provide proof on the existence of two different ligands, 2-pyridonate and 2-hydroxypyrimidine. As compared to 2-pyridone, only the most intense ring mode (1244 cm^{-1} in the spectrum of the free ligand) displayed what could be interpreted as a doubling of bands (1261, 1244 cm^{-1}) in **2**, yet none of the other ring modes did so.

We note that the NH$_3$ analogue of **2**, *trans*-[NH$_3$)$_2$Pt(C$_5$H$_4$NO)C$_5$H$_3$NO)]NO$_3$·2H$_2$O, **1**, according to IR-spectroscopy, does not display the same, very strong H bond (no unusual feature in the IR).

---

(19) Albert, A.; Sergeant, E. P. *The Determination of Ionization Constants*; Chapman and Hall: London, 1984; p 161.

(20) Schöllhorn, H.; Thewalt, U.; Lippert, B. *J. Am. Chem. Soc.* **1989**, *111*, 7213.

(21) Hollis, L. S.; Lippard, S. J. *Inorg. Chem.* **1983**, *22*, 2708.

(22) (a) Almlöf, J.; Kvick, A.; Olovsson, I. *Acta Crystallogr., Sect. B* **1971**, *B27*, 1201. (b) Penfold, B. R. *Acta Crystallogr.* **1953**, *6*, 591.

(23) Esd calculated according to $\sigma = (\sigma_1^2 + \sigma_2^2)^{1/2}$ with σ_1 and σ_2 being the errors in bond lengths and angles which are compared.

(24) For very short OH•••OH bonds (<2.5 Å), see: (a) Joswig, W.; Fuess, H.; Ferraris, G. *Acta Crystallogr., Sect. B* **1982**, *B38*, 2798 and references cited. (b) Olovsson, I.; Jönsson, P.-G. In *The Hydrogen Bond*; Schuster, P., Zundel, G., Sandorfy, C., Eds.; North-Holland Publ. Co.: Amsterdam, 1976; Vol. II, p 393 and references cited. (c) Emsley, J. *Chem. Soc. Rev.* **1980**, *9*, 91.

(25) Novak, A. *Struct. Bonding* **1974**, *18*, 177.

(26) (a) Hadzi, D.; Orel, B. *J. Mol. Struct.* **1973**, *18*, 227. (b) Hadzi, D.; Orel, B.; Novak, A. *Spectrochim. Acta, Part A* **1973**, *29A*, 1745.

(27) Lippert, B. *J. Raman Spectrosc.* **1979**, *8*, 274.

(28) (a) Lippert, B. *Inorg. Chem.* **1981**, *20*, 4326. (b) Pfab, R.; Jandik, P.; Lippert, B. *Inorg. Chim. Acta* **1982**, *66*, 193.

Table 6. Comparison of Selected Structural Features of 2-Pyridonate (L) and 2-Hydroxypyridine (LH) Ligands[a]

compd	N1−C2, Å	C2−O2, Å	O2−C2−N1, deg	N1−C2−C3, deg	ref
mer-$Pt(NH_3)_2Cl_3L$	1.397(8)[c]	1.266(8)[d]	121.4(6)[e]	116.6(6)[f]	21
cis-$[(NH_3)_2Pt(LH)_2]Cl_2$	1.335(9)[c]	1.340(9)[d]	115.2(7)[e]	121.0(7)[f]	21
trans-$[(CH_3NH_2)_2PtL(LH)]NO_3$ (**2**)	1.356(5)	1.302(5)	116.1(4)	119.8(4)	*b*

[a] Only those distances and angles are considered which are significantly different in the first two complexes (cf. ref 21). [b] This work. [c] Difference[23] corresponds to 5.2σ. [d] Difference[23] corresponds to 6.7σ. [e] Difference[23] corresponds to 6.9σ. [f] Difference[23] corresponds to 4.9σ.

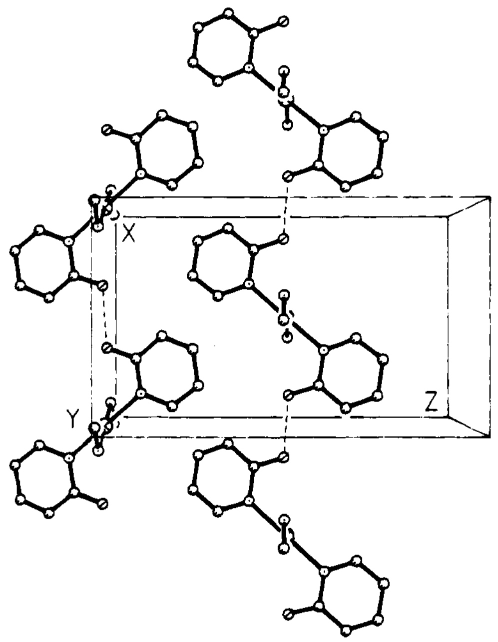

Figure 2. Section of packing of cations of **2** with very strong intermolecular H bond (2.443(9) Å) between cations indicated. Nitrates are omitted for clarity.

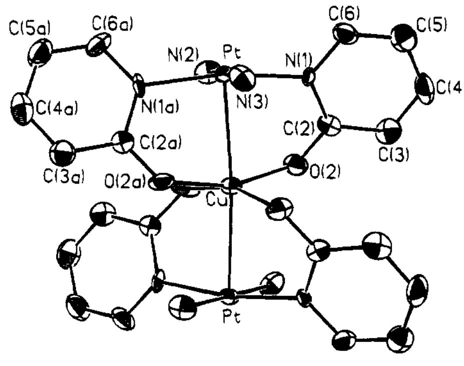

Figure 3. View of cation of *trans*-$[(NH_3)_2Pt(C_5H_4NO)_2Cu(C_5H_4NO)_2Pt(NH_3)_2](NO_3)_2$ (**3**) with atom-numbering scheme.

Crystal Structures of Pt_2Cu. Views of both trinuclear cations of **3** and **4** are given in Figures 3 and 4. In both cases the cations consist of two *trans*-(amine)$_2$Pt^{II} entities coordinating to the deprotonated ring nitrogens of *head−head* arranged 2-pyridone ligands and a Cu^{II} bound by the exocyclic oxygens of the four heterocyclic rings. In the case of **3**, Cu sits on a 2-fold axis in between the Pt's, forming an angle of 173.0(1)° with the latter. Bond lengths and angles are listed in Tables 7 and 8. Planes and deviations of atoms as well as packing diagrams are given in the supplementary material.

(i) Pt Coordination Spheres. In both compounds, the Pt coordination spheres deviate markedly from ideal square-planar. Distortion is such that Cu pushes Pt out of its N_4 plane. For example, in **3** Pt is approximately 0.09 Å away from the coordination plane defined by atoms N(1), N(2), N(1a), N(3), forming an angle of 170.5(4)° with N(1) and N(1a). In **4**, the corresponding angles are 174.9(2)° for Pt1 and 174.3(2)° for Pt2. At least for **3**, these angles are at the upper limit of deviations from ideal 180° in complexes of *trans*-a_2Pt^{II}.[9,10,29] Pt-N distances in **3** and **4** are normal.

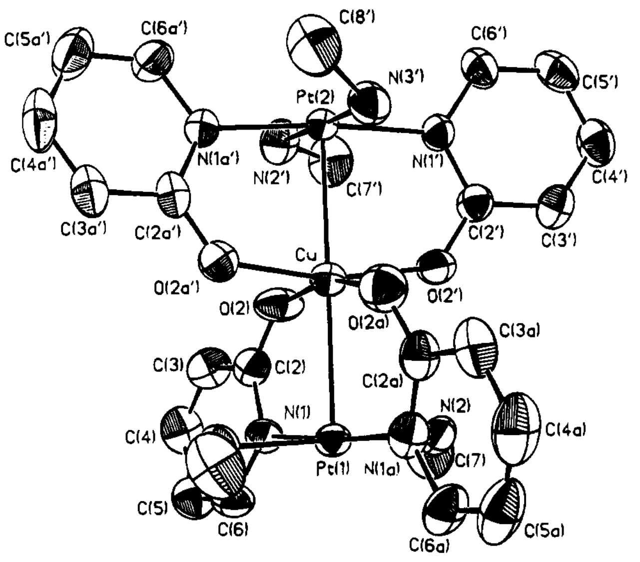

Figure 4. View of cation of *trans*-$[(CH_3NH_2)_2Pt(C_5H_4NO)_2Cu(C_5H_4NO)_2Pt(CH_3NH_2)_2](NO_3)_2$ (**4**) with atom-numbering scheme.

Table 7. Selected Bond Distances (Å) and Angles (deg) for Cation **3**[a]

Pt−Cu	2.6312(4)	Cu−Pt−N1	84.3(3)
Pt−N1	2.016(9)	Cu−Pt−N1a	86.4(3)
Pt−N1a	2.033(9)	Cu−Pt−N2	88.5(3)
Pt−N2	2.04(1)	Cu−Pt−N3	90.3(3)
Pt−N3	2.02(1)	N1−Pt−N1a	170.5(4)
Cu−O2	1.951(9)	N1−Pt−N2	90.8(4)
Cu−O2a	1.969(9)	N1−Pt−N3	88.7(4)
O2−C2	1.30(2)	N1a−Pt−N2	90.9(5)
O2a−C2a	1.27(2)	N1a−Pt−N3	89.3(5)
O3−N4	1.23(2)	N2−Pt−N3	178.7(4)
O4−N4	1.22(2)	Pt−Cu−Pt*	175.3(1)
O5−N4	1.24(2)	Pt−Cu−O2	81.4(3)
N1−C2	1.35(2)	Pt−Cu−O2a	80.7(2)
N1−C6	1.36(2)	Pt−Cu−O2a*	96.0(2)
N1a−C2a	1.40(2)	O2−Cu−O2a	162.1(3)
N1a−C6a	1.32(2)		
C2−C3	1.41(3)		
C2a−C3a	1.41(2)		
C3a−C4a	1.36(2)		
C3−C4	1.37(2)		
C4−C5	1.38(2)		
C4a−C5a	1.38(2)		
C5−C6	1.36(2)		
C5a−C6a	1.36(2)		

[a] For a complete list of angles and symmetry operations see supplementary material.

(ii) Cu Coordination Spheres. The Cu geometries in both compounds is best described as a slightly distorted, very flattened tetrahedron or alternatively as a strong distorted square

---

[29] Krizanovic, O.; Sabat, M.; Beyerle-Pfnür, R.; Lippert, B. *J. Am. Chem. Soc.* **1993**, *115*, 5538.

Table 8. Selected Bond Distances (Å) and Angles (deg) for Cation of **4**[a]

Pt1–Cu	2.6450(8)	Cu–Pt2–N3′	85.3(2)
Pt1–N1	2.030(5)	N1a′–Pt2–N1′	174.3(2)
Pt1–N1a	2.029(5)	N1a′–Pt2–N2′	88.0(2)
Pt1–N2	2.059(4)	N1a′–Pt2–N3′	91.3(2)
Pt1–N3	2.060(5)	N1′–Pt2–N2′	94.7(2)
Pt2–Cu	2.6320(8)	N1′–Pt2–N3′	86.1(2)
Pt2–N1a′	2.032(5)	N2′–Pt2–N3′	178.8(2)
Pt2–N1′	2.023(4)	Pt1–Cu–Pt2	175.17(3)
Pt2–N2′	2.054(5)	Pt1–Cu–O2′	96.7(1)
Pt2–N3′	2.059(5)	Pt1–Cu–O2a	81.9(1)
Cu–O2′	1.972(4)	Pt1–Cu–O2	81.4(1)
Cu–O2a	1.983(4)	Pt1–Cu–O2a′	98.6(1)
Cu–O2	1.974(4)	Pt2–Cu–O2′	82.1(1)
Cu–O2a′	1.965(4)	Pt2–Cu–O2a	102.8(1)
		Pt2–Cu–O2	94.0(1)
Cu–Pt1–N1	87.7(1)	Pt2–Cu–O2a′	83.0(1)
Cu–Pt1–N1a	87.3(2)	O2′–Cu–O2a	90.1(2)
Cu–Pt1–N2	89.3(2)	O2′–Cu–O2	92.9(2)
Cu–Pt1–N3	90.7(2)	O2′–Cu–O2a′	164.2(2)
N1–Pt1–N1a	174.9(2)	O2a–Cu–O2	163.2(2)
N1–Pt1–N2	93.6(2)	O2a–Cu–O2a′	88.2(2)
N1–Pt1–N3	86.0(2)	O2–Cu–O2a′	93.3(2)
N1a–Pt1–N2	87.2(2)		
N1a–Pt1–N3	93.3(2)		
N2–Pt1–N3	179.6(2)		
Cu–Pt2–N1a′	86.6(1)		
Cu–Pt2–N1′	88.1(1)		
Cu–Pt2–N2′	95.6(1)		

[a] For complete lists of distances and angles see supplementary material.

plane.[30] In **3** two angles about the Cu^{II} are 162.1(3)° and four angles are close to 90°. The situation in **4** is similar with angles around 163° and 88–93°. Cu-O distances are within the range of related heteronuclear Pt$_n$Cu (n = 1, 2) compounds.[2-6]

(iii) Pt-Cu Distances. They are 2.6312(4) Å in **3**, and 2.6320(8) Å and 2.6450(8) Å in **4**. These intermetallic separations are considerably shorter than those in all structurally characterized Pt$_n$Cu (n = 1 or 2) compounds derived from *cis*-a$_2$Pt^{II}L$_2$ or *cis*-a$_2$Pt^{II}LL′ (2.681(1) Å,[5] 2.684(1) Å,[3] 2.693(1) Å,[6] 2.765(3) Å,[2] 2.9843(1) Å [4]).

(iv) N-O Bite Distances. They differ somewhat within the two compounds (e.g. **3**: 2.31 Å, ring 1; 2.33 Å, ring a; **4**: 2.29 Å, ring 1; 2.29 Å, ring a; 2.30 Å ring 1′; 2.31 Å ring 1a′, esds 0.01–0.02) as do Pt-O distances (e.t. **3**: Pt-O(2a), 3.02 Å; Pt-O(2), 3.03 Å; **4**: Pt(1)-O(2) 3.05 Å; Pt(1)-O(2a), 3.07 Å; Pt-(2)-O(2′), 3.07 Å; Pt(2)-O(2a′), 3.10 Å). However, similar and even larger variations in bite and Pt-O distances are also seen in *trans*-[(NH$_3$)$_2$Pt(1-MeU)$_2$Ag$_2$]$^{2+}$, 2.21–2.34 Å and 2.99–3.19 Å, respectively, and therefore are not considered unusual. With dinuclear Pt complexes containing *cis*-a$_2$Pt residues (a = NH$_3$ or a$_2$ = en),[21,31] NO bite distances of 2-pyridone are rather constant, 2.30–2.32 Å, however.

(v) Torsional Twists. Views along Pt-Cu vectors in **3** and **4** (supplementary material) show that 2-pyridone rings bound to the same Pt display a pronounced propeller-twist in the case of **3** (35.5°), which is very much reduced in **4** (16.7° for two rings bound to Pt(1); 23.9° for two rings bound to Pt(2)). As a consequence, NH$_3$ groups of two different Pt's in **3** are rotated with respect to each other by ca. 40°, whereas nitrogens of the methylamine ligands in **4** are only slightly rotated (16°). Comparison of respective figures (supplementary material) convincingly demonstrates how a rather minor change from NH$_3$ to NH$_2$CH$_3$ ligands at Pt has a major effect on the overall structure of the trinuclear cation.

(vi) Intramolecular H Bonds. Intracomplex distances between the amine nitrogens at Pt and the pyridone oxygens of the second Pt moiety in all cases are sufficiently short to assume hydrogen bonding between these sites. In **4**, four different separations are observed, which vary between 2.87(1) and 2.98(1) Å. In **3**, variations in distances are more pronounced, 2.90(1) and 3.13(1) Å.

Electronic Spectra. The electronic spectra of compounds **3** and **4** differ significantly from those reported previously[5,7] for the related compounds derived from the *cis*-a$_2$PtL$_2$ precursors. Whereas these exhibit three bands in the visible/NIR region, at ~8500, 11 500 and 14 500 cm^{-1}, the room temperature reflectance spectra of compounds **3** and **4** show two rather intense peaks (Figure 5a), these being at 7580 and 12000 cm^{-1} for the former, and 6760 and 11 470 cm^{-1} for the latter. Compound **4** has an additional weak shoulder at ~18 300 cm^{-1}, presumably due to a charge-transfer transition or a d–d transition associated with the Pt(II) ions, on the edge of very strong absorption above 20 000 cm^{-1}. The spectrum of a thin section cleaved from an arbitrary crystal face of compound **4** also has a shoulder in this region at low temperature (Figure 5b). Weak shoulders on the band at 7400 cm^{-1} in this spectrum (Figure 5b) are probably due to infrared overtones. The band positions at ~12 K (7200 cm^{-1}, 11 600 cm^{-1}, 11 830 cm^{-1}) are slightly higher in energy than those observed in the reflectance spectrum at room temperature.

The observed shift of the Cu d–d transitions to lower energy on going from the planar arrangement of ligand oxygen atoms of the previous compounds, to the distorted tetrahedral environment in compounds **3** and **4**, is analogous to that observed for similar distortions for complexes such as CuCl$_4^{2-}$ [32,33] though the presence of the axial Pt atoms in the present compounds vitiates a straightforward comparison. In contrast to the situation for the previous centrosymmetric complexes, in the D_{2d} point group appropriate to compounds **3** and **4** the electronic transitions to the ^{2}E(*xz*,*yz*) and ^{2}A$_1$(z^2) excited states are Laporte-allowed in (*xy*) and *z* polarization, respectively. The bands in the crystal spectrum of **4** are indeed polarized in the expected fashion (Figure 5b), so that they can confidently be assigned to transitions to these excited states. Presumably, the transition to the ^{2}B$_1$($x^2 - y^2$) state, which is Laporte-forbidden, is too weak to be resolved. It is also possible that the shoulder at 8900 cm^{-1} is due to this transition, though the ligand-field calculations imply a higher energy (10 400 cm^{-}1; see following section). EPR measurements indicated averaged *g*-values of 2.25 and 2.10 when the magnetic field was parallel to the polarization directions (I) and (II), respectively. From the molecular *g*-values $g_{\parallel}$ = 2.430 and $g_{\perp}$ ~ 2.08 (see following section) it follows that the *z* molecular projection associated with polarization (I) is significantly greater than that with (II). As the band at 7200 cm^{-1} is more intense in (I) than (II), while the reverse is true for the band at 11 700 cm^{-1}, the selection rules imply that the former is due to the transition to ^{2}A(z^2), and the latter to ^{2}E(*xz*,*yz*).

EPR Spectra. The Q-band EPR spectrum of a powder of compound **4** (Figure 6b) shows two well-resolved resonances characteristic of a **g**-tensor of tetragonal symmetry with $g_{\parallel}$ = 2.430, $g_{\perp}$ = 2.083. Both *g*-values are significantly greater than those reported previously[5] for the related Pt$_2$Cu complexes

---

(30) Hathaway, B. J. In *Comprehensive Coordination Chemistry*; Wilkinson, G.; Gillard, R. D., McCleverty, J. A., Eds.; Pergamon Press: Oxford, U.K., 1987; Vol. V, p 533.

(31) O'Halloran, T.; Mascharak, P. K.; Williams, I. D.; Roberts, M. M.; Lippard, S. J. *Inorg. Chem.* **1987**, *26*, 1261.

(32) Lever, A. B. P. *Inorganic Electronic Spectroxcopy*, 2nd ed.; Elsevier: Amsterdam, 1984; p 569.

(33) Maasabni, A. C.; Nascimento, O. R.; Halvorson, K.; Willett, R. D. *Inorg. Chem.* **1992**, *31*, 1779.

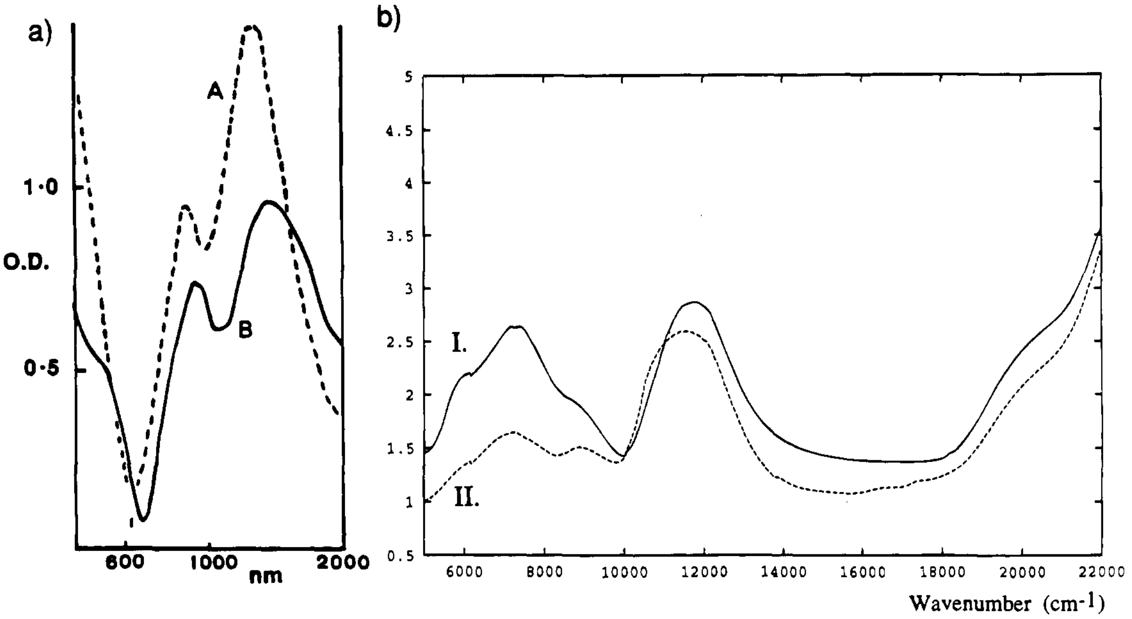

Figure 5. (a) Electronic reflectance spectra of (A) compound **3** and (B) compound **4**. (b) Electronic spectrum of an arbitrary crystal face of compound **4** measured at 12 K with the electronic vector along the two extinction directions (**I** and **II**).

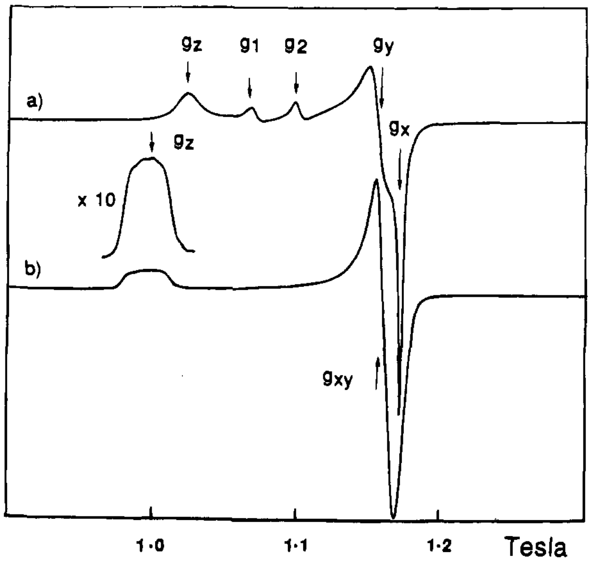

Figure 6. Room-temperature Q-band (33.88 GHz) spectra of polycrystalline samples of (a) compound **3** (receiver gain 6.3 × 10^3) and (b) compound **4** (receiver gain 1 × 10^4).

derived from the *cis*-a_2PtL_2 systems in which the CuO_4 units are planar (here, $g_{\parallel} \sim 2.37$, $g_{\perp} \sim 2.06$). Moreover, the spectrum of **4** suggests that there is an appreciable reduction in $A_{\parallel}$ to ca. 7.0 mT, resulting in a set of closely overlapping copper hyperfine components for the $g_{\parallel}$ band, in contrast to the $A_{\parallel}$ values of 10.85–12.38 mT observed for the compounds with planar CuO_4 units.[5,7] The increase in g-values and reduction in $A_{\parallel}$ on tetrahedral distortion of the CuO_4 units appears to parallel those noted previously for purely four-coordinate Cu(II) complexes.[34]

The spectrum of a powdered sample of **3** at Q-band is unusual (Figure 6a). In addition to the extrema associated with $g_{\parallel}$ and $g_{\perp}$ (g = 2.350 and ~2.08), weak peaks are observed at intermediate positions, g_1, g_2 as indicated by arrows on Figure 6a. The spectrum was essentially unchanged on cooling to 150 K. When taken in conjunction with the shoulder on the resonance due to $g_{\perp}$, the spectrum shows a superficial resemblance to that expected for a highly rhombic **g**-tensor with a significant copper hyperfine splitting associated with the middle g-value. This seems unlikely, as the complex shows no large geometric distortion away from tetragonal symmetry. A more plausible explanation is that a small fraction of the sample exhibits an "exchange-narrowed" **g**-tensor. Such a situation occurs for bis(methoxyacetato)$Cu^{II}(H_2O)_2$, Cu(methoxy)$_2(H_2O)_2$, which has[35] a powder EPR spectrum quite similar to that of compound **3**. Like **3**, Cu(methoxy)$_2(H_2O)_2$ has a basically tetragonal **g**-tensor, this having two different orientations in the unit cell. Under these circumstances, exchange-narrowed resonances occur at[35]

$$g_1 = (g_{\parallel} \cos^2 \alpha + g_{\perp} \sin^2 \alpha)$$

$$g_2 = (g_{\parallel} \sin^2 \alpha + g_{\perp} \cos^2 \alpha)$$

The third exchange-narrowed signal is at $g_{\perp}$, and 2α is the angle between the symmetry axes of the two **g**-tensors. The EPR spectrum of powdered Cu(methoxy)$_2(H_2O)_2$ consists of a basic pattern due to the molecular **g**-tensor, with weaker peaks corresponding to g_1 and g_2 which were assigned to an exchange narrowed **g**-tensor.[35] For compound **3**, $g_{\parallel} = 2.350$, $g_{\perp} \sim 2.08$, and substitution of the angle $\alpha = 41.5°$ indicated by the analysis of the single crystal EPR spectra (see below) yields the estimates $g_1 = 2.23$, $g_2 = 2.20$ for the exchange-narrowed g-values, in reasonable agreement with the values 2.26, 2.20 derived from the observed spectrum. This interpretation implies that the shoulder on the high-field resonance (Figure 6a) is due to a slight orthorhombic splitting of the $g_{\perp}$ component, rather than a hyperfine line ($g_{\perp} \rightarrow g_x = 2.067$, $g_y = 2.099$). In fact, the x axes of the **g**-tensors are parallel, so that for compound **3** it is g_y and g_z of the orthorhombic **g**-tensor which undergo exchange narrowing. Substituting the former for $g_{\perp}$, and the latter for $g_{\parallel}$ in the above equations, and allowing for an uncertainty of 2° in α and 0.002 in the g-values, yields the estimates $g_1 = 2.24 \pm 0.02$, $g_2 = 2.20 \pm 0.02$, which agree with the positions of the observed peaks within experimental uncertainty.

The X-band EPR spectrum of compound **3** (Figure 7) confirms the above interpretation. If the "anomalous" peaks were due to a hyperfine interaction, their separation should be

---

(34) See, e.g.: Yokoi, H.; Addison, A. W. *Inorg. Chem.* **1977**, *16*, 1341.

(35) Jakob, B.; Reinen, D. *Z. Naturforsch.* **1987**, *42b*, 1500.

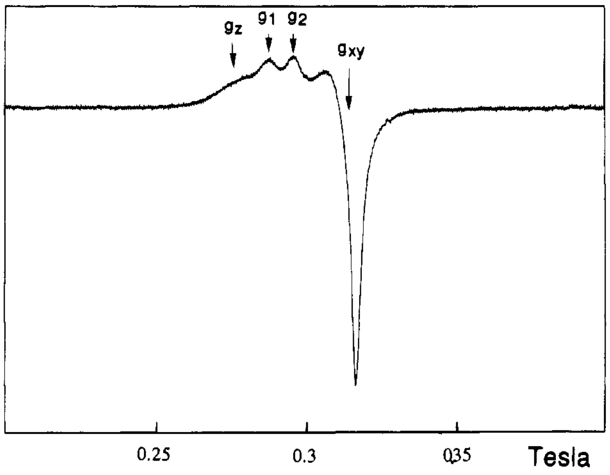

Figure 7. X-Band powder spectrum of compound **3**.

essentially independent of the microwave frequency, which is not the case. Instead, these peaks occur at magnetic fields corresponding to *g*-values identical to those at Q-band, as expected if they are due to an exchange-narrowed **g**-tensor. It is not clear why exchange-narrowing occurs for only a fraction of the sample, but this effect is expected when the exchange rate is comparable to the energy difference between the two signals, measured in frequency units.[36] This means that exchange-narrowing is more likely at X-band than Q-band, and in agreement with this, the "anomalous" lines are more prominent in the X-band spectrum (Figure 7). To further investigate this aspect, and better define the **g**-tensor of the complex, the EPR spectrum of a single crystal of **3** was studied. The *g*-values obtained at Q-band for rotations of the magnetic field about three orthogonal axes are shown in Figure 8. The definition of the angles indicating the orientation of the magnetic field, and the method of treating the data to obtain the molecular **g**-tensor, have been described previously.[37] Clearly resolved signals due to the two orientations of the complex were observed for those orientations for which two *g*-values are indicated on the figure. The signal due to each Cu was quite symmetical, and in no case was hyperfine structure observed. Similar results were obtained at X-band, except that the lower field dependence of the signals at this frequency meant that separate peaks could only be resolved over a narrow range of magnetic field orientations. The molecular *g*-values from the crystal measurements, $g_x = 2.069(4)$, $g_y = 2.096(3)$, $g_z = 2.350(4)$, with the uncertainties being shown in parentheses, are within experimental error identical to those obtained from the powder spectrum. The eigenvectors transforming these principal *g*-values into a molecular axis system defined with **x** bisecting the angle O2CuO2′, **z** normal to **x** and the Cu-Pt vector, and **y** normal to **x** and **z**, are as follows:

$$\begin{matrix} 0.997 & 0.082 & -0.010 \\ -0.083 & 0.994 & -0.066 \\ 0.004 & 0.066 & 0.998 \end{matrix}$$

The principal *g*-directions thus lie very close to the axes denoted by their subscripts, these coinciding with the axis system of the D_{2d} point group.

The g_z value of compound **3** is somewhat lower than that of **4**, and this is probably due partly to the fact that the excited states are slightly higher in energy in the former compound, leading to a smaller admixture of orbital momentum into the ground state. In addition, the fact that **3** has an orthorhombic **g**-tensor, while within experimental uncertainty **4** has a **g**-tensor of axial symmetry, will also lower the value of g_z for the former compound.[38]

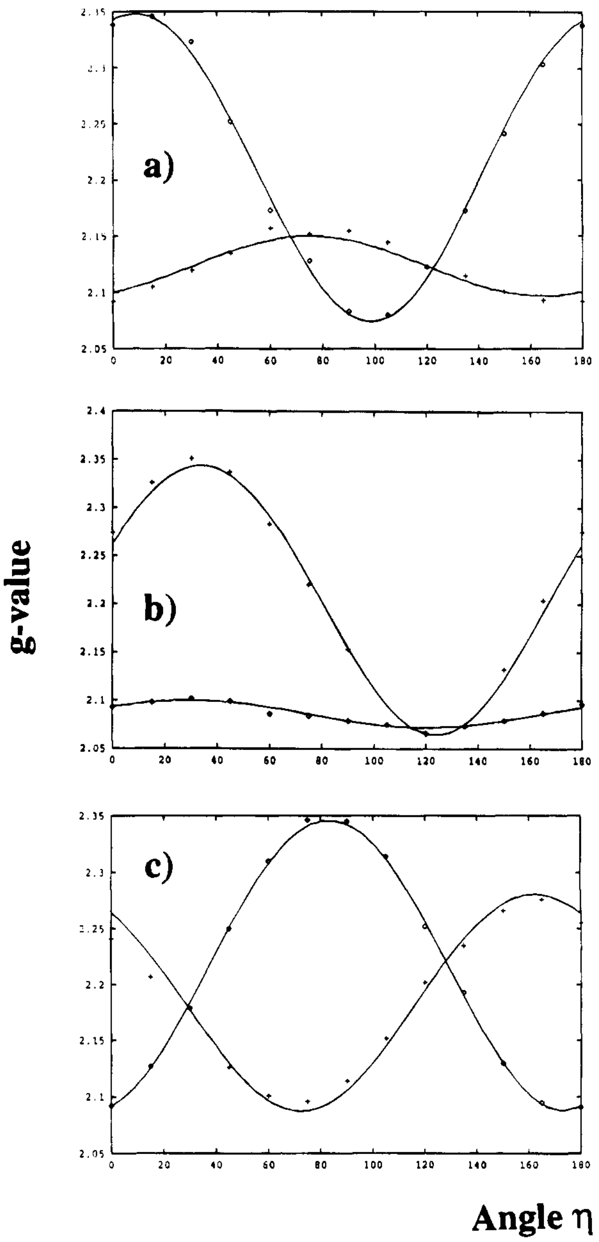

Figure 8. Measured *g*-values (symbols) obtained at Q-band for rotations of the magnetic field in three orthogonal planes of compound **3**, defined by angles (a) $\theta = 125.5°$, $\phi = 54.7°$, (b) $\theta = 135.0°$, $\phi = -90.0°$, and (c) $\theta = 69.5.5°$, $\phi = -22.3°$. The lines represent calculated values using the "best-fit" *g*-values; see ref 37 for the method of calculation and the definition of the angles defining the position of the magnetic field.

Metal–Ligand Bonding. The nature of the interaction between the Cu(II) atoms and the axial Pt^{2+} ions in these trimers is of particular interest. The previous analysis of the spectra of the trimers involving planar CuO_4 units suggested[7] that the axial Pt(II) atoms act as weak σ-donors toward the Cu(II) d-orbitals, behaving, in fact, in a manner very similar to a typical ligand such as chloride at a comparable bond length. This is perhaps surprising, in view of the formal positive charge on

---

(36) Abragam, A.; Bleaney, B. *Electron Paramagnetic Resonance of Transition Ions*; Clarendon Press: Oxford, U.K., 1970; p 57.

(37) Dawson, K.; Hitchman, M. A.; Prout, K.; Rossotti, F. J. C. *J. Chem. Soc., Dalton Trans.* **1972**, 1509.

(38) Hitchman, M. A. *J. Chem. Soc. A* **1970**, 4.

the Pt(II)—an electrostatic crystal-field model of the bonding would suggest that such a "ligand" should *stabilize* the Cu(II) d-orbitals *i.e.* that the Pt(II) should act as σ-acceptor "ligand". Analysis of the spectra of the present compounds provides further information on the bonding in this class of compound, and this is of particular importance as the electronic spectra could not be assigned unambiguously in the previous study.[7]

The bonding was modeled using the computer program CAMMAG developed by Gerloch and co-workers.[39] This represents the σ- and π-bonding interaction of each ligand in terms of parameters e_σ and e_π, with the overall energy levels of the complex being obtained by summing over all the ligands using the angular overlap matrix appropriate to the geometry of the complex revealed by its crystal structure.[40] The preferred assignment of the optical spectra of the previous complexes ($E(z^2) = {\sim}8500$, $E(xy) = 11\,500$ and $E(xz,yz) = 14\,500\ \text{cm}^{-1}$) yields bonding parameters $e_\sigma(xy) \sim 5885\ \text{cm}^{-1}$ and $e_\pi(xy) \sim 1600\ \text{cm}^{-1}$ for the oxygen ligands, and $e_\sigma(z) \sim 1580\ \text{cm}^{-1}$ for the effective σ-bonding parameter of the axial Pt(II) atoms. It should be noted that the latter includes both the direct σ-antibonding effect of the Pt(II) orbitals, and the effect of configuration interaction between the Cu(II) d_{z^2} and 4s orbitals.[41] Here, the Cu−O π-bonding was assumed isotropic about the bond axis, and the π-interaction due to Pt(II) atom was taken to be negligible. The Cu−O bond lengths (1.93, 1.99 Å) in one of the trimers containing planar CuO_4 units which formed the basis of the previous analysis, are quite similar to those in compound **3**, and the axial Cu−Pt distance (2.68 Å) is only marginally longer.[5] Assuming identical parameters for the metal−ligand interactions in the present complexes yields excited state energies in reasonable agreement with experiment. For compound **3** the calculated (observed) values in cm^{-1} are as follows:

$$E(z^2) = 8300\ (7600) \qquad E(xy) = 10\,700$$
$$E(xz,yz) = 13\,000,\ 13\,600\ (12\,000)$$

Here, a value of 590 cm^{-1} was used for the effective spin−orbit coupling constant. Virtually identical transition energies were calculated for compound **4** using these bonding parameters. An improved fit for compound **3** is obtained using slightly lower bonding parameters, $e_\sigma(xy) = 5250$, $e_\pi(xy) = 1200$, $e_\sigma(z) = 1350\ \text{cm}^{-1}$:

$$E(z^2) = 7500\ (7600) \qquad e(xy) = 10\,400$$
$$E(xz,yz) = 12\,000,\ 12\,600\ (12\,000)$$

If these bonding parameters are decreased slightly for compound **4** to take into account the slightly longer Cu−O bond distances by assuming an inverse dependence on the sixth power of the bond length, as done in previous studies,[42] to give $e_\sigma(xy) = 4975$, $e_\pi(xy) = 1140$, $e_\sigma(z) = 1350\ \text{cm}^{-1}$, good agreement with experiment is obtained for this compound also:

$$E(z^2) = 7000\ (7200) \qquad E(xy) = 9870$$
$$E(xz,yz) = 11\,570,\ 12\,140\ (11\,600,\ 11\,830)$$

The g-values estimated with CAMMAG using isotropic orbital reduction parameters $k = 0.80$ and 0.83 for compounds **3** and **4**, respectively, are also in reasonable agreement with experiment (values in parentheses): $g_x = 2.073\ (2.069)$, $g_y = 2.074\ (2.096)$, $g_z = 2.385\ (2.350)$ for **3** and $g_x = 2.079\ (2.083)$, $g_y = 2.082\ (2.083)$, $g_z = 2.437\ (2.430)$ for **4**. The marginally higher orbital reduction parameter for **4** is consistent with the slightly longer Cu−O bonds in this compound. While the calculated orientation of the g-axes for **3** is as observed, the in-plane g-anisotropy is smaller than that observed experimentally. The cause of this orthorhombic component is unclear. The effect of assigning different bonding parameters to the two oxygen atoms to take into account the slight inequivalence in the Cu−O bond lengths ($Cu{-}O_2 = 1.93$ Å, $Cu{-}O_{2a} = 1.98$ Å) in compound **3** was investigated, but the effect on both the g-values and the electron transition energies was insignificant. This is to be expected, since the long and short Cu−O bonds are trans to one another, so that the holohedrized symmetry[40] remains close to tetragonally symmetric.

The use in the present calculations of bonding parameters derived from the alternative assignment proposed[7] for the optical spectra of the trimers containing planar CuO_4 units produced very poor agreement with experiment, the ^2E state being misplaced by ${\sim}1500\ \text{cm}^{-1}$. The possibility that the Cu−O π-bonding is anisotropic was also investigated, but this also produced poorer agreement with the experimentally observed electronic transition energies.

Summary

2-Pyridone[43] and its C-substituted derivatives have been and are still widely applied as mono-[44] and bidentate[45] ligands, especially in Pt chemistry (Pt blues,[46] diplatinum(III) species[47]), and occasionally in mixed-metal systems.[48,49] The here described compounds **2**−**4** add two aspects to the chemistry of this ligand: First, the formation of a very short intermolecular hydrogen bond between N-metalated 2-pyridone and its protonated form, the 2-hydroxypyridine ligand, as observed in **2**, and second, heteronuclear Pt_2Cu complexes **3** and **4**, which display unexpectedly distorted coordination spheres of all three metals. As far as the Cu^{II} in **3** and **4** is concerned, its coordination geometry bears some relevance to an "entatic state" as seen in many metaloproteins.[50] From model building it would seem that a strictly parallel orientation of all three metals is possible in principle, with amine protons of Pt^{II} and oxygens of Cu^{II}

---

(39) Cruse, D. A.; Davies, J. E.; Gerloch, M.; Harding, J.; Mackey, D.; McMeeking, R. F. CAMMAG, a FORTRAN computing package, University of Cambridge, 1979.

(40) For a detailed description of the functioning of CAMMAG, see: Gerloch, M. *Magnetism and Ligand Field Analysis*; Cambridge University Press: New York, 1983.

(41) Smith, D. W. *Inorg. Chim. Acta* **1977**, *22*, 107.

(42) Astley, T.; Canty, A. J.; Hitchman, M. A.; Rowbottom, G. L.; Skelton, B. W.; White, A. H. *J. Chem. Soc., Dalton Trans.* **1991**, 1981.

(43) Concerning the minor tautomer, 2-hydroxypyrimidine, see, e.g.: (a) Beak, P. *Acc. Chem. Res.* **1977**, *10*, 186 and references cited. (b) Bensaude, O.; Chevrier, M.; Dubois, J. E. *J. Am. Chem. Soc.* **1978**, *100*, 7055. (c) Schlegel, H. B.; Gund, R.; Fluder, E. M. *J. Am. Chem. Soc.* **1982**, *104*, 5347 and references cited.

(44) See, e.g.: (a) Reedijk, J. *Recueil* **1969**, *88*, 1140. (b) Reedijk, J. *Recueil* **1972**, *91*, 681.

(45) See, e.g.: (a) Cotton, F. A.; Ren, T.; Eglin, J. L. *Inorg. Chem.* **1991**, *30*, 2552 and references cited. (b) Rodman, G. S.; Mann, K. R. *Inorg. Chem.* **1988**, *27*, 3338. (c) Clegg, W.; Garner, C. D.; Akhter, L.; Al-Samman, M. H. *Inorg. Chem.* **1983**, *22*, 2466.

(46) See, e.g.: (a) O'Halloran, T. V.; Mascharak, P. K.; Williams, I. D.; Roberts, M. M.; Lippard, S. J. *Inorg. Chem.* **1987**, *26*, 1261. (b) Ginsberg, A. P.; O'Halloran, T. V.; Fanwick, P. E.; Hollis, L. S.; Lippard, S. J. *J. Am. Chem. Soc.* **1984**, *106*, 5430 and references cited. (c) Barton, J. K.; Rabinowitz, H. N.; Szalda, D. J.; Lippard, S. J. *J. Am. Chem. Soc.* **1977**, *99*, 2827.

(47) See, e.g.: (a) Peterson, E. S.; Bancroft, D. P.; Min, D.; Cotton, F. A.; Abbott, E. H. *Inorg. Chem.* **1990**, *29*, 229 and references cited. (b) O'Halloran, T. V.; Roberts, M. M.; Lippard, S. J. *Inorg. Chem.* **1986**, *25*, 957. (c) Hollis, L. S.; Roberts, M. M.; Lippard, S. J. *Inorg. Chem.* **1983**, *22*, 3637. (d) Hollis, L. S.; Lippard, S. J. *Inorg. Chem.* **1983**, *22*, 2605.

(48) Wang, S.; Trepanier, S. J.; Wagner, M. J. *Inorg. Chem.* **1993**, *32*, 833.

(49) Berardini, M.; Emge, T. J.; Brennan, J. G. *Inorg. Chem.* **1993**, *32*, 2724.

(50) We are, of course, aware that this analogy does not apply to the donor atoms typically found in metaloproteins.

being strongly hydrogen bonded (N••O ≈ Pt−Cu ≈ 2.6 Å). This is not realized in these compounds, however. Likewise, an analogous dinuclear structure as found in mixed PtPd[9] and PtHg[10] complexes containing two *trans*-bridging 1-methylcytosinato (1,5-dimethylcytosinato) nucleobases, is not observed, even though in this system, Cu^{II} behaves in a similar fashion as do Pd^{II} and Hg^{II}.[51] Thus the structural features of **3** and **4** extend the list of binding patterns[8−10] seen in heteronuclear complexes derived from *trans*-a_2PtL_2.

Acknowledgment. This work has been supported by the Deutsche Forschungsgemeinschaft (DFG), the Fonds der Chemischen Industrie (FCI), and Asta Medica. We thank A. Erxleben for her help in the preparation of the figures.

Supplementary Material Available: Tables of complete crystallographic data, anisotropic displacement parameters, and calculated positional parameters for H atoms for **2−4**, bond angles for **3** and **4**, bond distances for **4**, and torsional angles for **3** and **4**, packing diagrams for **2−4**, and ORTEP views of cations **3** and **4** along the Pt−Cu axis (24 pages). Ordering information is given on any current masthead page.

---

[51] Fusch, G.; Fusch, E. C.; Lippert, B. Unpublished results.